As originally published in the SMTA Proceedings.

Pad-to-Pad Electrical Field Effects on Surface Insulation Resistance

David Lober, Mike Bixenman, D.B.A., Mark McMeen
Magnalytix
TN, USA
dlober@magnalytix.com

ABSTRACT
From the development of Surface Insulation Resistance (SIR) an emphasis has been placed on utilizing a few "standard" test patterns, namely the "Y" test pattern, and interdigitated "comb" patterns. These designs have historically lagged "leading edge" PCB design rules, and even typical PCB design rules. These patterns share a common feature, in that they are "spherical cows", meaning that they are a highly simplified model of a complex phenomenon. The long, uniformly spaced, parallel electrode shape of the "Y" and "comb" patterns allows for the assumption of a uniform electric field. This means that the force imparted on an ion between the test patterns is independent of where it is located. However, this approximation is not valid when applied to modern components.

"Real" footprints of modern components have complex geometries which violate these assumptions. This may lead to certain areas underneath a component to experience higher electric fields, meaning ionic contamination is subjected to greater forces, leading to increased ElectroChemical Migration (ECM) risk. Newer SIR test patterns are starting to use real component footprints as the basis for their design. In this paper, which is the first in a series of examining the relationship between SIR, ECM, and SIR test patterns, we examine the effect that various design factors of SIR test patterns has on the electric field on the surface of the PCB.

Key words: Insert here to aid in searches.

INTRODUCTION
Cleanliness Test Methods
When it comes to measuring the cleanliness of PCBs there are three main methods in use in the high reliability electronics industry: Resistance Of Solvent Extract (ROSE), Ion Chromatography (IC), and Surface Insulation Resistance (SIR). There are additional methods, such as Fourier Transform Infrared Spectroscopy (FR-IR) or Scanning Electron Microscopy-Energy Dispersive Spectroscopy (SEM-EDS), which are general surface analysis techniques but are usually only employed in specific situations, typically root cause failure analysis, and certainly don't have widespread use as a process control technique.

Resistance of solvent extract
ROSE is the oldest of the three common methods used in high reliability electronics, and was developed by the U.S. Navy's Naval Avionics Facility in 1972[1], and gaining wide spread use by around 1983[2]. Briefly, ROSE attempts to correlate the change in electrical conductivity of a mixture of 2-propanol (also known as isopropyl alcohol or IPA) and DI water to an equivalent mass of sodium chloride per unit of PCB surface area.

However, ROSE was developed to solve a *specific* problem, measuring highly ionic rosin fluxes on 1970s vintage through hole electronic soldered with tin-lead solder, which is a problem that does *not* exist in modern electronics manufacturing. Despite these limitations being initially identified in the mid to late 1980s, see Ellis as an example[3] as the industry shifted from large through hole components to smaller SMT technology, and again in the late 1990s as the industry shifted away from rosin fluxes to no clean fluxes which have limited solubility in IPA and DI water, and yet again in the mid-2000s as REACH and RoHS drove the industry towards halide free and lead free solder flux and alloys , ROSE has persisted. For a more complete picture of ROSE testing, it's advantages, it's failures, and it's history a prior article by Lober may be a good starting point[4].

Ion Chromatography
IC can be considered a more sophisticated version of ROSE testing, in that it still (attempts) to dissolve contamination in an IPA/DI water mixture and detects the contamination via conductivity of a solution, and thus inherits the same problems as ROSRE testing. However, in between these steps the contamination flows through a chromatographic column, which separates charged species based off of their electrostatic affinity towards the stationary phase. This separation stage, when done properly, can allow for the identification and quantification of individual ionic species present. IC has had a low adoption rate in the industry, due to the specialized nature of the chromatography system. New IC systems routinely cost in excess of $75,00 USD, and generally require a chemist to at least commission the IC if not to operate it and interpret the data. Furthermore, while the identification and quantification of ionic species gives information about the relative risks of the contamination, translating this data into the absolute risk of the contamination on the reliability of the PCB is difficult if not impossible to ascertain.

SIR
SIR is the "odd man out" of the three main cleanliness test methods, in that it is the only one that attempts to directly relate the level of contamination on a PCB to an electrical property, the resistance of the surface of the PCB.In the

standard SIR test an InterDigitated Electrode (IDE) is used, generally referred to a "comb pattern", is created on a standardized PCB, such as IPC-B-52, IPC-B-24, or others. A generalized diagram of a comb pattern is shown in Figure 1. The key parameters are generally considered to be the width of the individual electrodes, W, and the gap between them, G. The width of the electrodes, in conjunction with the gap spacing, dictates the number of electrodes that can be fit into the available PCB surface area. However, the primary parameter that many are interested is in, is G, as it determines the electric field strength.

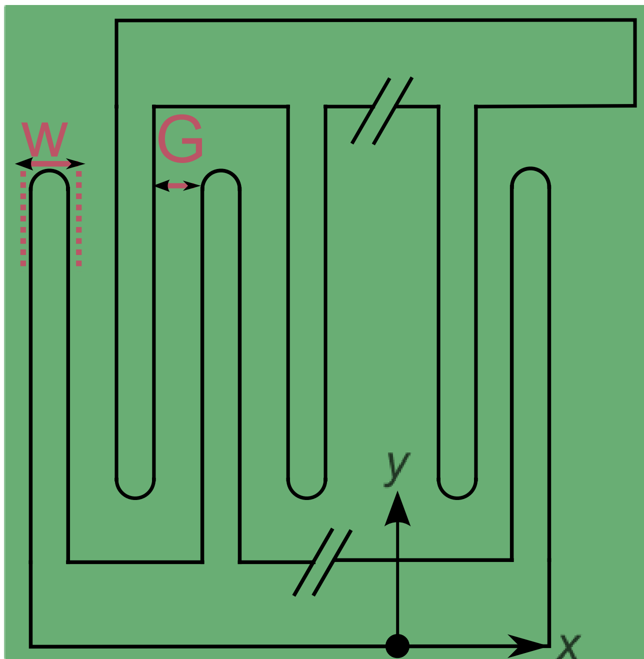

Figure 1: Schematic of a comb pattern

Spherical Cows

In physics, it is not uncommon to simplify a complex problem by making an approximation. An often-used approximation in naive physics is a "spherical cow", in which one assumes a cow is a perfect sphere, In the development of SIR comb patterns the electric field between the electrodes were treated as a spherical cow.

The "spherical cow" approximation made in the development of SIR testing is that the comb pattern can be modeled as an ideal electrostatic field. For this idealized electric field to exist there are two electrodes which are perfectly parallel, perfectly smooth, of infinite length, and the space in between the electrodes is of homogenous composition. With this approximation, the formula for the electric field between the electrodes is given as:

(1.1) $$E = \frac{V}{d}$$

where V represents the voltage and d is the linear distance, and historically the electric field has been recommended to be 25 V/mm. The electric field can be imagined as the force that is acted upon a "test charge", a small positive charge that does not influence the electric field A more complete method of calculating the electric field is by solving the Laplace equation for electric potential (1.2).

(1.2) $$-\nabla \cdot \varepsilon \nabla \Phi = 0 \quad \in \Omega$$

Only one of these approximations holds true for comb patterns, infinite length, as the length of the comb is long enough to be considered infinite from the standpoint of ions present on the PCB. Traces on PCBs are not perfectly smooth lines, they have a surface roughness, which distorts the electric field. Furthermore, the space between electrodes are not made up of a homogenous material. Solder mask, inks, conformal coatings, flux residue, are just a few of the various materials which may be between electrodes in a real-world case. Furthermore, in practice electronics do not consist of perfectly parallel traces, they are comprised of component footprints or even distributed circuit elements. This negates the concept of uniform electric fields.

The last "spherical cow" is an often overlooked one, that is SIR testing is monitoring *electrochemical* processes, ion migration and leakage currents. As Bagotsky puts it *"Classical electrostatics deals with the interactions of idealized electric charges. Electrochemistry deals with real charged particles having both electrostatic and chemical properties.[5]"* The mechanism of SIR (leakage currents) and ECM consists of complex electrochemical processes which are not well understood.

Electric Fields

The focus on electric fields is twofold. First, if we assume that the resistance and the distribution of contamination is equivalent between two geometries of test patterns, then the leakage current which drives SIR will be greatest along the path with the highest electric field. Secondly, the leakage current is not purely electrical in nature, it is electrochemical. The ionic contamination present on a PCB can migrate in an electric field, increasing the leakage current and causing ECM or dendritic growth to occur. The current carried by these ions is proportional to the area, the ionic mobility (μ), the ion charge (z) and the electric field (1.3). This means that when the electric field is increased in SIR testing, ion migration needed for certain electrochemical failure mechanisms will be increased.

(1.3) $$i \propto |z| A \mu \frac{V}{d}$$

METHODS

General

Two different designs of SIR patterns were examined, both theoretically and experimentally. The first design was an interdigitated comb pattern based off of the IPC-B-53 design, designated MGX-53, shown in the Appendix as Figure 2. MGX-53 consists of four quadrants of interdigitated electrodes which each have a different combination of number of combs, gap width (G), and comb width (W) given in Table 1. One feature of note is the two horizonal traces above and below the comb pattern. The purpose of these

traces is to allow for a glass cover to be soldered to the PCB to simulate the presence of a component over the comb pattern.

Table 1: MGX-53 Design Parameters

Quadrant	Electrodes	Width (mm)	Gap (mm)
A	50	0.41	0.51
B	40	0.41	0.40
C	35	0.32	0.32
D	50	0.41	0.20

The second PCB design, designated as QFN-48 consisted of four quadrants containing four identical QFN-48 footprints connected in parallel. Each quadrant had a different combination of pad width (equivalent to "W" in Figure 1) and pad gap (equivalent to "G" in Figure 1).

Table 2: QFN-48 Design Parameters

Quadrant	Width (mm)	Gap (mm)
A	0.20	0.30
B	0.25	0.25
C	0.30	0.20
D	0.35	0.15

FEM

A two stage approach was used in FEM modeling a course modeling phase and a fine modeling phase, due to the relatively long length of the electrodes in relationship to the interelectrode distance. In course modeling stage for the FEM analysis all eight (8) of the different test patterns were modeled in CAD. This model was then converted into a 2D mesh using GMSH and Delaunay triangulation[6]. In this phase the 2D mesh consisted of around $1x10^6$ elements. Next the electric field was modeled using ElmerFEM[7]. The Laplace equation,(1.2), was solved for electrical potential. A fixed potential difference of 5 VDC was applied between pairs of electrodes. The derived electric field was averaged over elements, rather than the more accurate and complex Galerkin method. ParaView was used for visualizing the results[8].

For the fine modeling stage, the test pattern was simplified to allow closer examination of the electric fields without substantially increasing computational time. For the MGX-53 patterns only three electrodes were modeled, and the length of the electrodes was substantially reduced. For the QFN-48 only four pads were examined. The density of the mesh was then increased by an order of magnitude ($\sim 1x10^7$ 2D elements)

SIR

To further understand the effects that the test pattern design has on the SIR values an experimental Design Of Experiment (DOE) was conducted, Table 3. Four variables were of interest to this DOE: populated, flux type, electrode type, and electrode design. The first three variables are standard two level factors, the fourth variable (electrode design) is a compounded variable. The levels for electrode design are the same ones given in Table 1 and Table 2. For the unpopulated PCBs the designated solder flux was printed on the test pattern, however no simulated component was placed over the test pattern. The SIR test conditions were a bias and measurement voltage of +5 VDC, a temperature of 40 ºC and a relative humidity of 90%.

Table 3: DOE for experimental portion

Variable	Description	Levels
Populated	Is there a difference in SIR/ECM between populated and unpopulated test patterns?	TRUE FALSE
Flux type	Is there a difference in SIR/ECM between a rosin or no clean flux?	Rosin No Clean
Electrode Type	Is there a difference between IDE and QFN-48 test patterns for SIR/ECM?	IDE QFN-48
Electrode Design	What effects does changing the electrode width (W) and gap (G) have on SIR/ECM?	8 levels (see Table 1, Table 2)

Results

FEM

After the submission of the abstract for this paper a paper using similar methods was published in 2021 by Reiss, et al.. [9]. Reiss, et al. used FEM analysis to investigate the effects of surface roughness on ECM, not SIR specifically. Their results substantiate the results of this work. In Reiss, et al. they found that increasing the roughness of the copper and the copper prepreg interface caused an increase in the electric field and a decrease in the time to failure for ECM.

Due to space constraints only the FEM results for the QFN-48 pattern and the IDE pattern at a spacing of 0.2 mm (7.874 mil) will be presented, the others are available upon request. Unless noted otherwise, the reported electric fields values are for the magnitude of the electric field.

The high-resolution FEM calculation of the electric field for a QFN with 0.2 mm pad spacing is shown as Figure 4. As expected for a bias of 5 V and a gap of 0.2 mm most of the inter-electrode area has an electric field magnitude of 25 V/mm which is an industry standard. There are two features to note in the structure of the electric field. First, the electric field is most intense at the corners of the pad. This is to be expected and is caused by the sharp corners of the pad. This results in a region of electric field to be greater than 50 V/mm which would exhibit twice the force on an ion in that region as opposed to along the edges of the pad. Secondly, the pads which are on the outside only have strong electric fields on

the inside edges of the pads, as they are facing a pad with a different potential.

Figure 5 shows an overview for the calculated electric field for the equivalent IDE pattern. The electric field magnitude is mapped to the same color scheme as for the QFN pattern. Figure 7 shows the distance between an area of high electric field and its counter electrode. To better illustrate the regions of various electric fields, see Figure 8 and Figure 9.

SIR
SIR values for the last two hours of the 168 hour test were averaged for both the MGX-53 (IDE) SIR pattern and the QFN-48 test pattern. This average was used to conduct a Type II ANOVA analysis. **Error! Reference source not found.** contains the data for the QFN-48 SIR data and Table 4 for the MGX-53 data.

Table 4: ANOVA for QFN-48 DOE

Variable	Sum Sq	Df	F value	Pr(>F)
Populated	**12.40**	**1**	**48.74**	**0.00**
Design	0.35	3	0.46	0.71
Flux Type	**1.50**	**1**	**5.90**	**0.02**
Populated Design Interaction	0.54	3	0.71	0.55
Populated Flux Type Interaction	0.03	1	0.13	0.72
Design Flux Type Interaction	0.15	3	0.20	0.90
3 Way Interaction	0.03	3	0.04	0.99
Residuals	11.70	46		

For the MGX-53 test PCB all main effects were statistically significant at the $p<0.05$ level, and no interactions were significant. For the QFN-48 only populated and flux type were statistically significant.

Table 4: ANOVA for MGX-53 DOE, no interactions were significant

Variable	Sum Sq	Df	F value	Pr(>F)
Populated	**127.3**	**1**	**217.09**	**0.00E+00**
Design	**8.8042**	**3**	**5.00**	**3.73E-03**
Flux Type	**6.9755**	**1**	**11.90**	**1.05E-03**
Residuals	34.012	58		

Due to space constraints the tables of the regression coefficients are in the figures section. Table 5 contains the regression coefficients for QFN-48 design. Going from an unpopulated QFN-48 SIR test pattern to a populated one decreased the SIR value by 0.86±0.348 $\log_{10}\Omega$, which is substantially larger than the effect of changing flux type had. Table 6 contains the estimate of the regression coefficients for the MGX-53 design. For this SIR test pattern the effect that populating the test pattern had was much greater than that for the QFN-48 design. Populating the IDE pattern caused a reduction of the SIR value by -282±0.382 $\log_{10}\Omega$. The next largest effect was the distance between electrodes when going from G=0.32 mm to G=0.20 mm.

CONCLUSIONS
The goal of this paper is to start transitioning the industry from a spherical cow, to a cylindrical one. We are not attempting to create a comprehensive model of SIR, but we are attempting to improve the current model.

FEM
From the FEM analysis of the electric field distribution of the IDE and the QFN electrode configurations the following conclusions can be made:

1. QFN electrode configurations have a greater maximum electric field magnitude than IDE electrode configurations.
    a. This should result in higher ion migration rates, causing a decrease in time until failure and/or lower SIR.
2. IDE electrode designs create isolated regions of high electric field magnitude, where as QFN electrodes create two areas of high electric field strength in proximity to each other, maximizing the ion migration rate.
3. For both IDE and QFN electrodes the optimal pattern from an electric field standpoint has the greatest ratio of inner electrodes to outer electrodes; for both IDE and QFN electrodes having a single row of electrodes instead of two rows of electrodes maximized the amount of force experienced by ions in between the electrodes.

SIR
From the analysis of the SIR data the following conclusions and inferences can be drawn:

1. A QFN-48 SIR test pattern has a lower SIR value than a IDE pattern
2. For the QFN-48 SIR pattern populating the test pattern with a QFN-48 component was the most substantial effect study in reducing the SIR value
    a. Presumably the presence of the component will not effect the 3D structure of the electric field.
    b. It is presumed that the presence of the component reduces the amount of solvent from the flux that volatilizes off during reflow yielding ions which are more mobile
3. For the MGX-53 (IDE) test patter population was the greatest factor influencing SIR
    a. Going from a gap of 0.32 mm to 0.20 mm between adjacent electrodes had the only statistically significant spacing effect
    b. Flux type had a slightly significant impact on SIR
4. The discrepancy between the reduction in SIR values that occurred from populating the MGX-53

design vs the QFN-48 design may be due to differences in outgassing the solder flux solvent
   a. The MGX-53 design has a greatly increased thermal mass when compared to the QFN-48 design
   b. The QFN-48 design has a shorter distance for the volatilized flux solvents to travel before being vented than the MGX-53 design
5. The MGX-53 was the only design that had a statistically significant change in SIR value based off of the gap between electrodes. This effect was only seen in going from a gap of 0.32 mm to 0.20 mm.

REFERENCES

[1] W. Hobson, "Printed-Wiring Assemblies; Detection of Ionic Contaminants on," NAVAL AVIONICS FACILITY INDIANAPOLIS IND, Materials Research Report 3-72 (1972), 1972.

[2] D. Sanger and K. Johnson, "A Study of Solvent and Aqueous Cleaning of Fluxes.," NAVAL WEAPONS CENTER CHINA LAKE CA, 1983. [Online]. Available: https://apps.dtic.mil/sti/citations/ADA124950

[3] B. N. Ellis, "Contamination Control: Quo Vadis?," *Circuit World,* vol. 12, no. 4, pp. 40-43, 1986, doi: 10.1108/eb043835.

[4] D. Lober, M. Bixenman, M. McMeen, Z. Papiez, T. Forsythe, and C. Anthony, "Cleanliness Detection and Resistance of Solvent Extract – A Critical Evaluation," presented at the SMTAI, Minneapolis, 2021.

[5] V. S. Bagotsky, *Fundamentals of Electrochemistry*. Wiley, 2005.

[6] C. Geuzaine and J.-F. Remacle, "Gmsh: A 3-D finite element mesh generator with built-in pre- and post-processing facilities," *International Journal for Numerical Methods in Engineering,* vol. 79, no. 11, pp. 1309-1331, 2009, doi: https://doi.org/10.1002/nme.2579.

[7] I. Kondov and G. Sutmann, "Multiscale modelling methods for applications in materials science," Jülich Supercomputing Center, 389336899X, 2013.

[8] J. Ahrens, B. Geveci, and C. Law, *ParaView: An End-User Tool for Large Data Visualization* (Visualization Handbook). Elsevier, 2005.

[9] G. Reiss, B. Kosednar-Legenstein, J. Riedler, and W. Eßl, "Impact of electric field at rough copper lines on failure time due to electrochemical migration in PCBs," *Microelectronics Reliability,* vol. 117, p. 114035, 2021/02/01/ 2021, doi: https://doi.org/10.1016/j.microrel.2021.114035.

APPENDIX

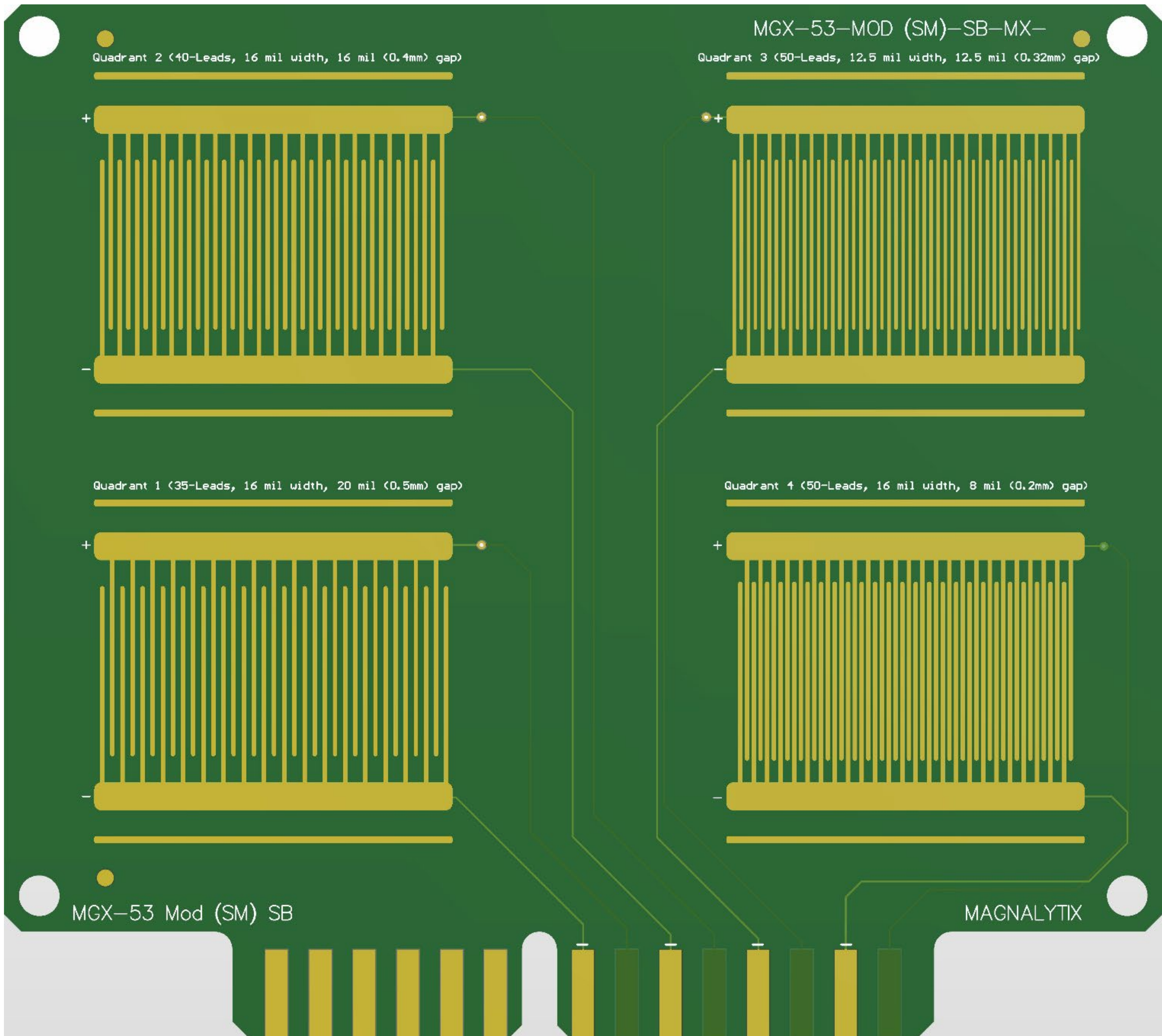

Figure 2: MGX-53 PCB design

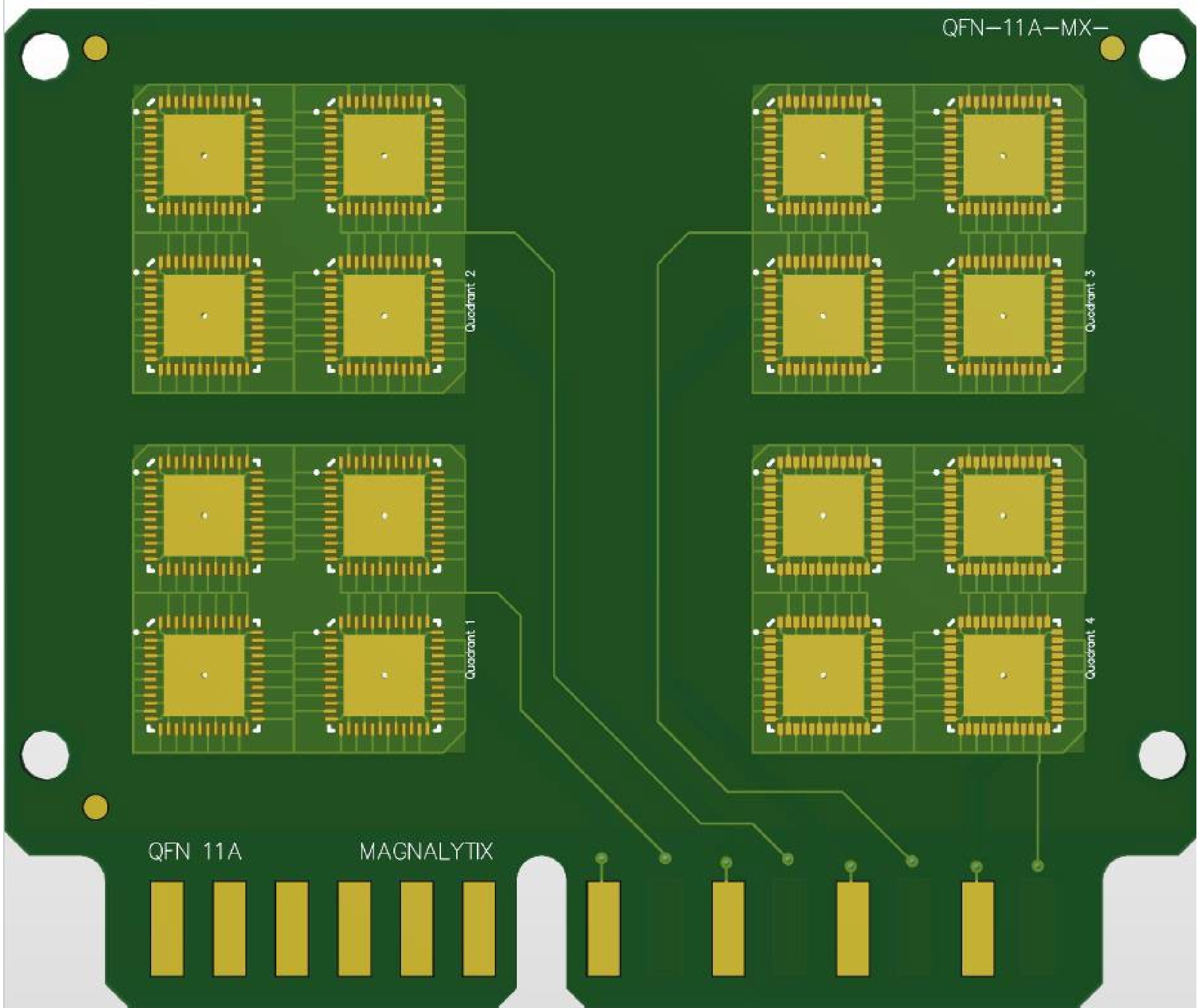

Figure 3: QFN-48 PCB design

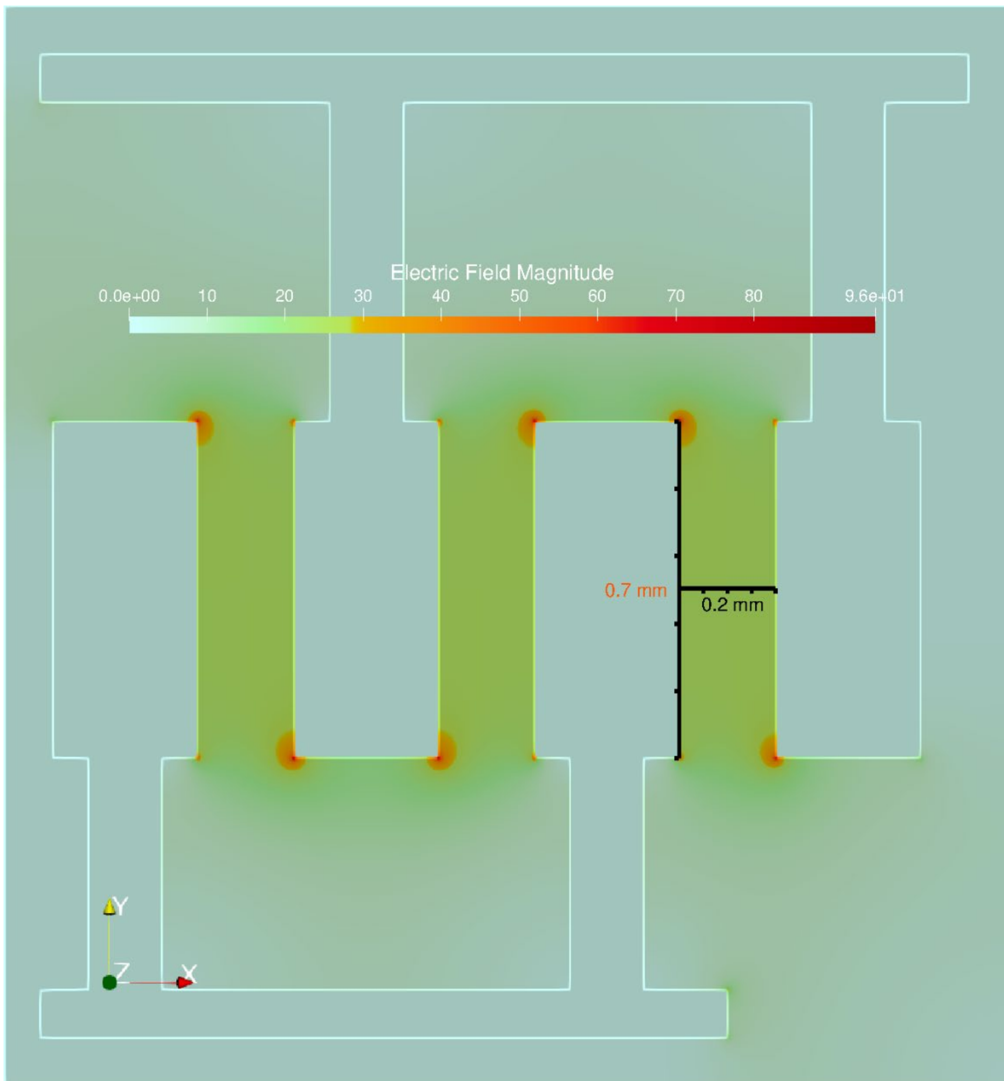

Figure 4: QFN-48 detailed electric fields

Figure 5: Electric fields for IDE pattern

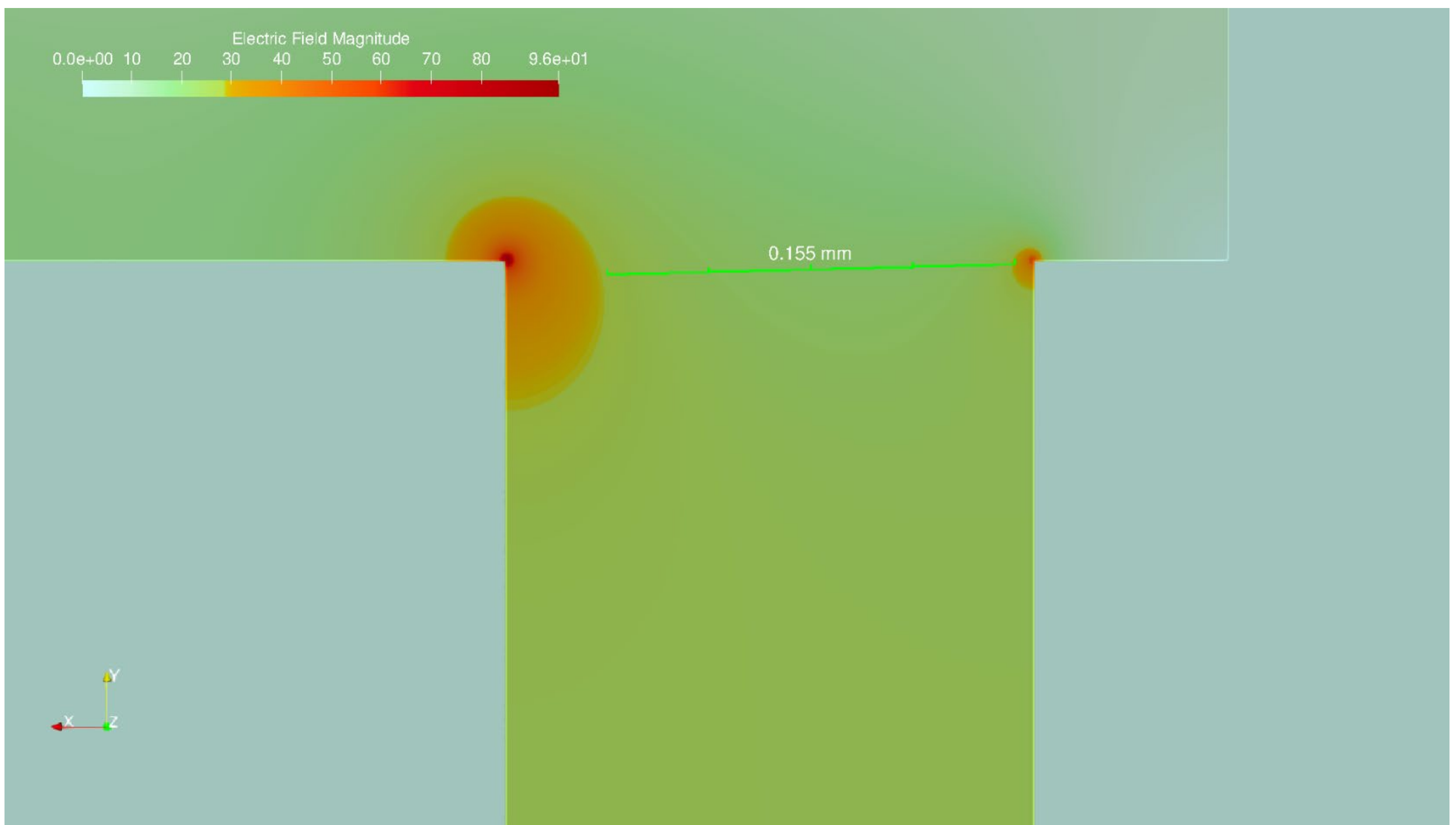

Figure 6: QFN-48 High electric field separation.

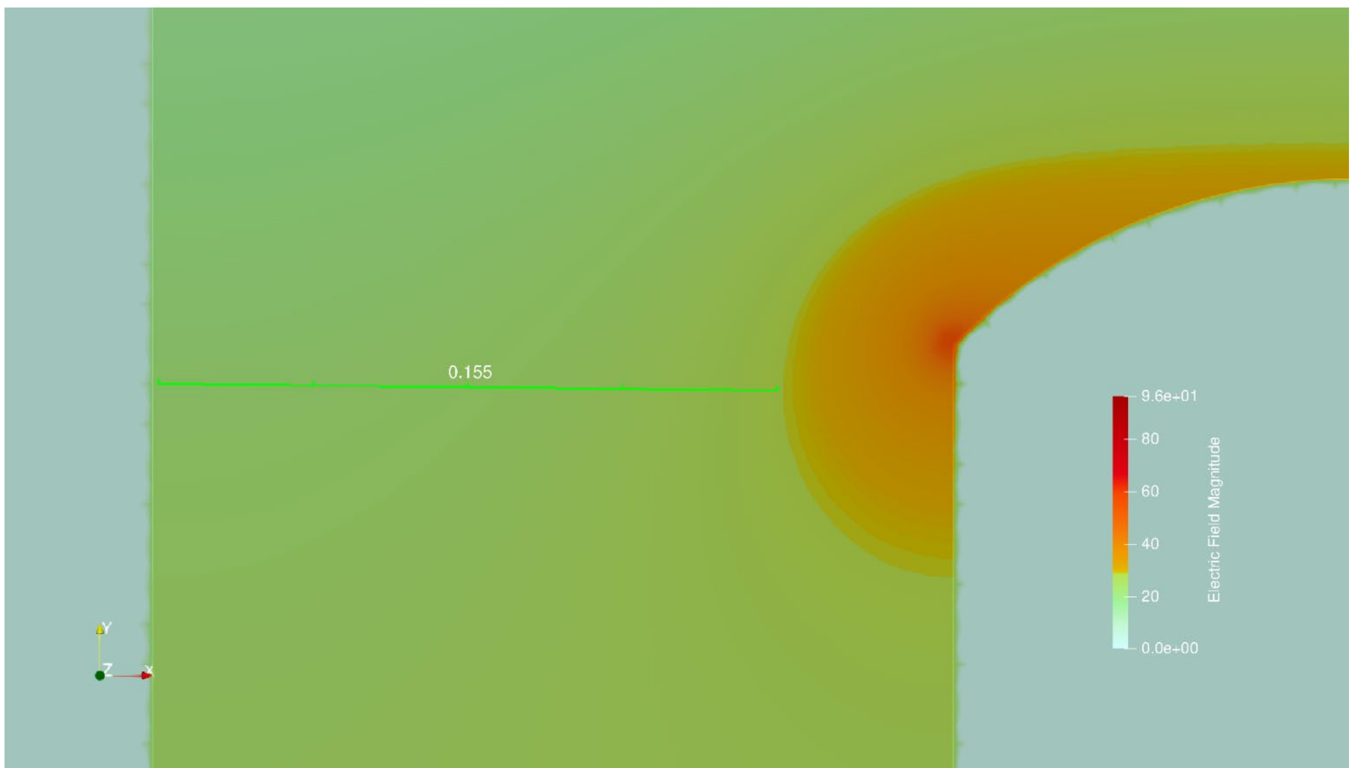

Figure 7: High electric field magnitude separation IDE.

Figure 8: QFN pattern electric field regions.

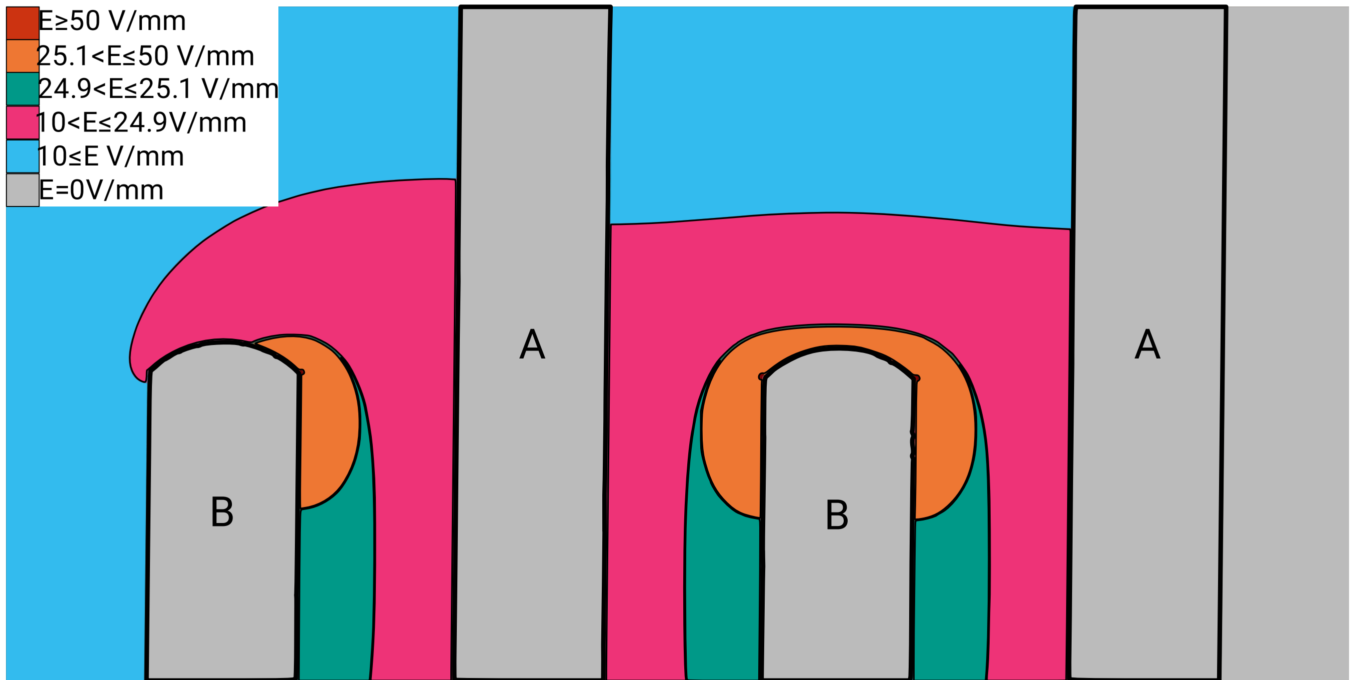

Figure 9: IDE pattern electric field regions. A: Electrode body; B: Electrode tips; Note dimensional scale is different than **Figure 8**

Table 5: QFN-48 Regression Coefficients

Term	Coefficient estimate	S.E.	95% Confidence Interval		F statistic	DF	p Value
			Low	High			
Intercept	**10.22**	**0.117**	**9.98**	**10.45**	**87.10**	**58**	**3.48E-63**
Populated=TRUE	**-0.86**	**0.172**	**-1.20**	**-0.52**	**-5.01**	**58**	**5.45E-06**
Flux=Rosin	**0.35**	**0.166**	**0.02**	**0.68**	**2.13**	**58**	**0.037684**
Flux=Rosin; Populated=TRUE	-0.08	0.239	-0.56	0.40	-0.34	58	0.732625

Table 6: MGX-53 Regression Coefficients

Term	Coefficient estimate	S.E.	95% Confidence Interval		F statistic	DF	p Value
			Low	High			
(Intercept)	**12.34**	**0.234**	**11.87**	**12.81**	**52.64**	**58**	**1.16E-50**
Populated=TRUE	**-2.82**	**0.191**	**-3.20**	**-2.48**	**-14.73**	**58**	**2.90E-21**
G=0.4 mm	-0.18	0.271	-0.73	0.36	-0.68	58	5.00E-01
G=0.32 mm	-0.27	0.271	-0.81	0.27	-1.01	58	3.18E-01
G=0.2 mm	**-0.98**	**0.271**	**-1.52**	**-0.48**	**-3.61**	**58**	**6.35E-04**
Flux=Rosin	**-0.66**	**0.191**	**-1.04**	**-0.28**	**-3.45**	**58**	**1.05E-03**